Performance Evaluation of Bifacial PV Systems in Distribution Networks Operation: A CVR Study Considering Smart PV Inverter Control

Mojtaba Ahanch
Department of Electrical Engineering
University of Arkansas
Fayetteville, AR 72701, USA
mahanch@uark.edu

Roy McCann

Department of Electrical Engineering

University of Arkansas

Fayetteville, AR 72701, USA

rmccann@uark.edu

Mahdi Rouholamini

Department of Electrical and Computer Engineering

Wayne State University

Detroit, MI 48202, USA

gj9598@wayne.edu

Caisheng Wang

Department of Electrical and Computer Engineering

Wayne State University

Detroit, MI 48202, USA

cwang@wayne.edu

Abstract—Compared to a conventional mono-facial photovoltaic (PV) module, a bifacial one is more efficient as it receives light from not only the front but also the backside. The daily irradiance profile of a bifacial PV module is of a two-peak trajectory that almost coincides with the morning and evening peak demands. This interesting property helps distribution network operators better handle the issues caused by the abundance of conventional PVs during midday (i.e., Duck curve). Moreover, this two-humped profile can be incorporated into network operation strategies such as conservation voltage reduction (CVR). Thus, this paper proposes a new CVR framework that best uses the double-peak profile of bifacial PV modules to improve the voltage profile of a distribution network. The proposed framework optimally coordinates legacy voltage control devices, including on-load tap changers and voltage regulators, as well as Volt/VAr control of smart inverters. The effectiveness of the proposed framework is simulated and verified on the well-known modified 34-bus system using the Matlab-COM-OpenDSS platform. The results clearly demonstrate the advantages of bifacial PVs over their mono-facial counterparts.

Keywords—Bifacial PV modules, CVR, OpenDSS, Smart inverter, Volt/VAr control

I. INTRODUCTION

Utilities carry out CVR strategies on their distribution feeders for peak load shaving and energy conservation through the voltage reduction of voltage-sensitive customers. CVR can be fulfilled using the conventional operation of legacy voltage control devices such as on-load tap changers (OLTC), automatic voltage regulators (VRs), capacitor compensators (CAPs), or advanced integration of CVR into Volt/VAr optimization (VVO) models [1]. Considering today's high penetrations of PVs, researchers have proposed novel combinations of CVR and

The authors express their gratitude to the funding provided to support this study from National Science Foundation (NSF) EPSCoR RII Track-2 Program under the grant number OIA-2119691. The findings and opinions expressed in this article are those of the authors only and do not necessarily reflect the views of the sponsors.

Volt/VAR control (VVC) to keep the system operation voltage within its permissible band. For instance, Ding [2] evaluated the impacts of two different smart PV inverter functions on the CVR benefit. The authors coordinated the aggregated reactive power and autonomous Volt/VAR control of smart PV inverters with conventional voltage regulating devices. In [3], an event-driven predictive method was introduced for real-time VVO and CVR implementation in different operational time scales by considering unforeseen uncertainties in PV power generation and load demands.

In [4], Hossan proposed an integrated CVR and demand response framework considering different stochastic-based scenarios for modeling customer-end distributed energy resources (DER) and loads. The centralized OPF-based CVR with high PV penetrations proposed in [5] is modeled as a nonlinear programming problem that can effectively handle the scalability issues caused by the discrete variables. A risk-based energy management algorithm is proposed in [6], which uses both load shifting and CVR to minimize energy costs with regard to the uncertainties of PV generation. In [7], Singh proposed a time horizon-based predictive VVO that can operate in centralized and local control modes. Separating the combined VVC/CVR problem into two sub-problems is a viable solution that has been successful in prior studies. The researchers in [8] proposed a two-layer local real-time adaptive VVC capable of minimizing voltage oscillations and dynamically adapting the control parameters while facing substation voltage changes and PV output uncertainties. In [9], the authors presented a bi-level VVO approach to coordinate the legacy voltage control devices with smart PV inverters. In [10], a new two-stage framework was proposed for the optimal coordination of the battery energy storage system (BESS) and the soft open point (SOP) devices while implementing the demand response program (DR) and CVR schemes.

In [11], a multistage coordinated CVR approach was introduced to incorporate inverter-based distributed generators (IDGs) and SOP devices for online and offline stages. The

proposed stochastic CVR considers the intermittency and uncertainties of both load demand and generations, and the model-predictive control is used for the offline stage. In a similar study, a multistage multi-objective Volt/VAR strategy maximizes the CVR economic benefits through slow and fast time scale controllers [12]. To mitigate the voltage fluctuations, an adaptive Volt/VAR droop-controlled method was employed for fast time controllers. In [13], the authors proposed a new integrated Volt/VAR and CVR method aiming at minimizing voltage deviations, improving energy conservation, and reducing the legacy device operation. The equilibrium optimization algorithm (EOA) was used to solve the multiobjective optimization problem. The proposed framework in [14] coordinates BESS, legacy devices, and smart PV inverters to minimize substation demand and power loss. The authors implemented the arithmetic optimization algorithm (AOC) in a MATLAB-COM-OpenDSS platform to find the optimal solutions. Standard mono-facial PVs have been the subject of the studies. However, due to the remarkable achievements in solar cell technology, bifacial PV modules might soon be considered an alternative to their mono-facial counterparts. It is said that the goal of an under \$1/Watt total system price by 2030 [15] is achievable if bifacial PVs are used. Bifacial technology is going to make up around 30% of the market by 2027 [16]. Thus, this paper investigates the impacts of bifacial systems on distribution network operation by focusing on a CVR study. The rest of this paper is organized as follows: Section II introduces the bifacial PV modeling. The proposed framework is discussed in section III, and the simulation results will be presented in section IV. Finally, Section V concludes the paper.

II. BIFACIAL PV MODELING

Thanks to the recent development in solar panel technologies, bifacial PV panels are now gaining considerable attention from researchers and industries. Compared to monofacial PV technologies and their pertinent control strategies (which have been widely investigated by researchers around the world [17-19]), bifacial panels generate additional power while the panel dimensions are preserved. The additional power is produced via better using the sky diffused, and ground reflected light [20]. In addition to boosting the output power, the bi-sided nature of bifacial PV panels helps generate more appealing daily energy profiles [21]. Fig. 1 illustrates an overview of how bifacial PV modules use the sky diffused and ground reflected light.

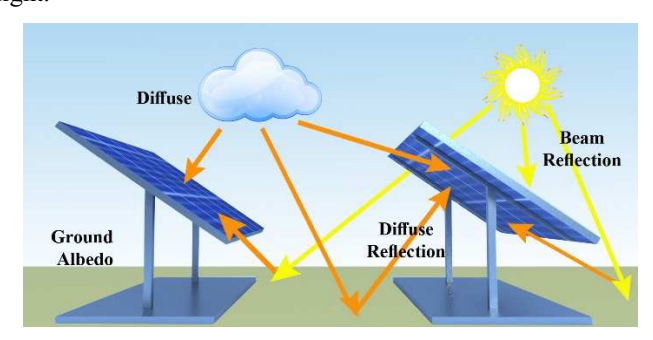


Fig. 1. Bifacial PV modules with diffused, scattered, and reflected light.

A few researchers have investigated the energy yield of bifacial PV panels considering various installation parameters such as tilt angle, clearance from the ground, and ground albedo, each of which can significantly impact the performance of bifacial panels [22]-[23]. In [24], the authors proposed a new incident energy-based framework for the optimal modeling and configuration of fixed multi-row bifacial PVs. They included in their study the site-related parameters, such as the tilt and orientation angles, the horizontal distance between the PV rows, the array's height off the ground, and the ground reflection coefficient. They evaluated the impacts of the aforesaid aspects on their proposed bifacial model. In this study, the model given in [24] will be employed to simulate the bifacial system we have used in our CVR strategy.

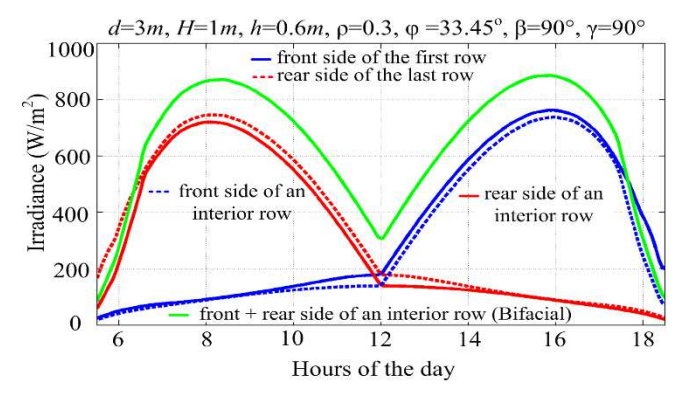


Fig. 2. Irradiance incident on an east-west vertically aligned bifacial plant in Phoenix, AZ (July 22).

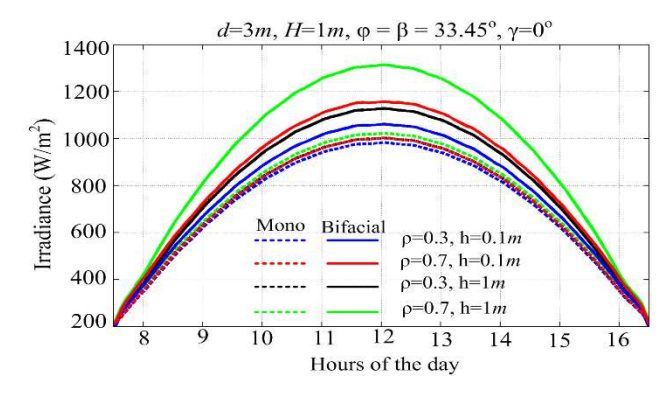


Fig. 3. Irradiance incident on an interior row of a south-facing bifacial plant in Phoenix, AZ (in the Winter solstice).

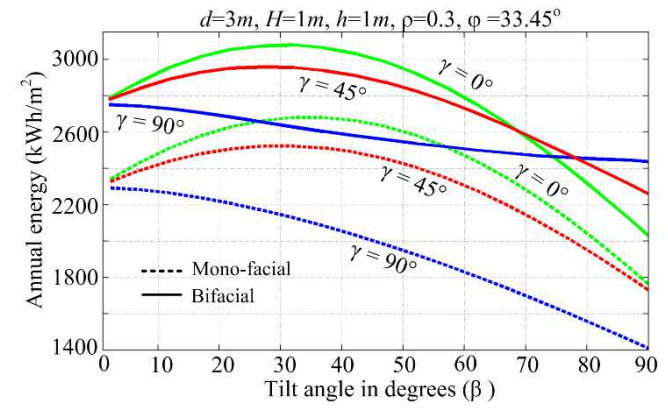


Fig. 4. Impacts of various tilt and orientation angles on the annual energy incident on an interior PV row (for a site located in Phoenix, AZ).

Fig. 2 depicts the solar irradiance incident on the front and rear sides of a random middle as well as an exterior (very first or very last) PV row. From Fig. 2, it can be observed that the irradiance reaching a bifacial array may possess a double-peak profile whose humps almost coincide with morning and evening peaks in electricity consumption. Such a two-humped generation profile can significantly benefit distribution network expansion which later on will be discussed in this paper.

An interesting question associated with the performance of bifacial panels is how much the produced power could increase if a mono-facial PV array were literally replaced with a bifacial array while the array's configurations are kept the same. The question has been well answered in [24]. Fig. 3 shows the solar irradiance incident on an interior row of the system under study. As it can be noticed, the obtainable irradiance has increased by 9% while the ground was covered with concrete (ρ =0.3), and the array is slightly elevated (h=10cm). It is evident that the irradiance is escalated by around 18% as the ground was fully covered by snow (ρ =0.7). The figure also displays the effects of elevating the bifacial PV panels. As seen in Fig. 3, elevating the panels from h=10cm to h=1m will cause the aforesaid increments to be 16% and 31%, respectively. As mentioned earlier, the tilt and orientation angles remarkably affect the irradiance received by a bifacial PV module. Fig. 4 depicts the annual energy incident on a yearly basis on an interior PV row in terms of various tilt and orientation angles when ρ =0.3 and h=0.1m. As seen in Fig. 4, the solar energy reaching a bifacial PV array is always greater than its corresponding mono-facial one, no matter how tilted the array is. Furthermore, the tilt angle at which maximum annual energy can be obtained (the optimal tilt angle) varies with regard to the changes in the orientation angle: nevertheless, the obtainable maximum energy associated with the optimal tilt angle is nearly constant. This indicates that different bifacial PV configurations lead to approximately the same quantity of maximum yearly energy. Such flexibility will grab PV system designers an additional freedom degree when configuring a bifacial PV farm.

III. THE PROPOSED FRAMEWORK

A. CVR problem

In this subsection, the proposed CVR strategy is defined as a mixed-integer nonlinear multi-objective optimization problem (MINLP), which also takes into account the constraints associated with power flow balance and transmission limitation.

$$Minimize \left(SS_{Energy} + VD\right). \tag{1}$$

In the above objective function, *VD* is the voltage deviation on distribution feeders defined as follows:

$$VD = \frac{1}{nb} \sum_{i \in nb} (1 - \mu_i) \tag{2}$$

$$\mu_{i} = \begin{cases} \frac{V_{i} - V_{\min}}{V_{n} - V_{\min}} & if & V_{\min} \leq V_{i} \leq V_{n} \\ \frac{V_{\max} - V_{i}}{V_{\max} - V_{n}} & if & V_{n} \leq V_{i} \leq V_{\max}, \end{cases}$$
(3)

where, V_n and V_i are the nominal voltage and the i^{th} bus voltage, respectively. Equation (3) indicates that the closer the values of μ_i are to 1, the smaller the voltage deviation would be. The second objective function (4), which must be minimized, represents the amount of energy received from the substation.

$$SS_{Energy} = \sum_{time=1}^{t} \sum_{i=1}^{n} kW_{SSdemand}^{t} = \sum_{time=1}^{t} \sum_{i=1}^{n} kW_{Load}^{t} + kW_{Loss}^{t}$$
 (4)

$$kW_{Load}^{t} = \sum_{\varphi = a,b,c} \sum_{m=1}^{nl} (P_{Lm}(V_{m}))_{\varphi}^{t}$$
 (5)

$$kW_{Loss}^{t} = \sum \left(P_{Line-loss}^{t} + P_{Transformer-loss}^{t} + P_{Inv-loss}^{t} \right) \tag{6}$$

$$P_{Line-loss} = \sum_{i=1}^{N} \sum_{j=1, \ i \neq i}^{N} R_{ij} * I_{ij}^{2}$$
 (7)

$$I_{ij} = (|V_i| \angle \delta_i - |V_j| \angle \delta_j) * |Y_{ij}| \angle \theta_{ij},$$
(8)

Where, $kW_{SSdemand}$, kW_{Loss} , and kW_{Load} are the substation power demand, active power loss, and active load, respectively. Also, $P_{Line-Loss}$, $P_{Transformer-loss}$, $P_{Inv-loss}$ denote the line loss of the network, transformer total loss, and PV inverter loss, respectively.

$$P_i = P_{Gi} - P_{Li} = \sum_{i=1}^{N} \left| V_i V_j Y_{ij} \right| \cos \left(\theta_{ij} + \delta_j - \delta_i \right)$$
(9)

$$Q_{i} = Q_{Gi} - Q_{Li} = \sum_{i=1}^{N} |V_{i}V_{j}Y_{ij}| \sin(\theta_{ij} + \delta_{j} - \delta_{i})$$
 (10)

$$V_i^{Min} \le V_i \le V_i^{Max} V_i^{Min} = 0.95 \, pu, V_i^{Max} = 1.05 \, pu,$$
(11)

where, P_{Gi} and P_{Li} are the generated and load active power, Q_{Gi} and Q_{Li} are the generated and load reactive power, and V_i denotes the voltage of each node.

B. Line Drop Compensation (LDC) approach

In this study, the LDC approach is applied to the voltage regulating devices, including OLTC and VRs, to regulate the voltage throughout the distribution feeder. Hence, the voltage drop is computed considering the measured line current, resistance, and reactance.

The required tap positions are calculated, and the device is then adjusted accordingly to compensate the voltage drop [25]:

$$R_{Comp_{\Omega}} + X_{Comp_{\Omega}} = (R_{Line_{\Omega}} + X_{Line_{\Omega}}) \cdot \frac{CT_p}{N_{PT} \cdot CT_s} \Omega, \quad (12)$$

where, R_{Line} and X_{Line} are the line resistance and reactance, respectively. CT_P , N_{PT} , and CT_S denote the primary current transformer, turn ratio, and secondary current transformer, respectively. The compensator R and X settings are calibrated in Volts using the following equation:

$$R' + jX' = (R_{Comp_{\Omega}} + X_{Comp_{\Omega}}).CT_{s}.$$
 (13)

C. OLTC and VRs modeling

The equations below generalize the regulation procedure for the OLTC and VRs [26]:

$$b_{vr} = 1 + Tap_{vr} \times \frac{\Delta V_{step}}{100} \tag{14}$$

$$\Delta V_{step} = \left(\frac{S \tan dard \ Voltage \ \text{Re} \ gulation}{No \ of \ steps}\right), \tag{15}$$

where, b is the voltage regulation ratio of regulating device. For the OLTC:

$$b_{OLTC} = \pm 10\%,$$

 $Taps = [-16,...0,...,16]$
 $\Delta V_{step} = 0.625\%,$ (16)

and for the VRs:

$$b_{VRs} = \pm 5\%,$$

 $Taps = [-8,...0,...,8]$ (17)
 $\Delta V_{step} = 1.25\%.$

$$\sum_{time=1}^{t} TapChange_{vr}^{t} \leq TapChange_{vr}^{\max}.$$
 (18)

D. PV inverter control mechanism

The Volt/VAr scheme is utilized in this study to define the compensating reactive power that smart PV inverters can provide. Fig. 5 shows the Volt/VAr curve. The four parameters of the curve (P_1 to P_4) are determined based on the voltage relations expressed in (19).

$$Q = \begin{cases} Q^{\text{max}} & V < V_1 \\ \left(\frac{V_1 - V}{V_2 - V_1}\right) * Q^{\text{max}} & V_1 < V < V_2 \\ 0 & V_2 < V < V_3 \\ \left(\frac{V_3 - V}{V_4 - V_3}\right) * Q^{\text{max}} & V_3 < V < V_4 \\ -Q^{\text{max}} & V > V_4. \end{cases}$$

$$(19)$$

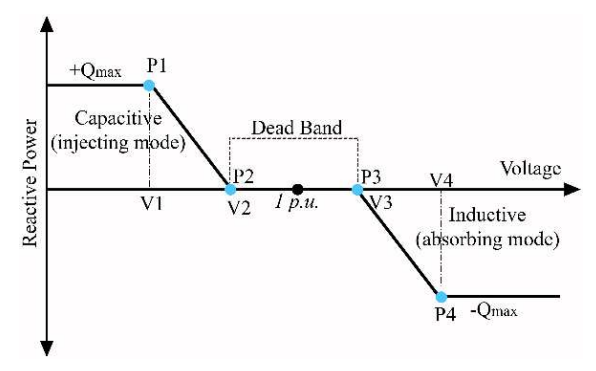


Fig. 5. Volt-VAr characteristics of smart PV inverters.

IV. SIMULATIONS AND DISCUSSIONS

A. The case study

The proposed framework is tested on the modified 34-bus system using a Matlab-COM-OpenDSS platform. The test system is modeled in OpenDSS, and the PSO algorithm is run in MATLAB. Also, The COM interface makes a connection between MATLAB and OpenDSS which facilitates the data transfer (including the set points for the OLTC, VRs, and PV inverters as well as power flow results such as node voltages and lines currents). The case study distribution network (shown in Fig. 6) consists of a 2.5 MVA substation transformer with an OLTC, two VRs, and two bifacial PV systems. While the OLTC regulates the voltage at the substation, the VRs are in charge of voltage regulation throughout the feeder. Considering the LDC method introduced in the preceding section, V_{reg} of the OLTC and VRs is set to 120V. Moreover, delays of 30 and 45 seconds are applied for the OLTC and VRs, respectively. The maximum allowable tap change of each voltage regulating device is 1 step in each data acquisition interval for PV plants and loads (every 15 minutes). Furthermore, by implementing the Volt/VAr characteristic scheme, bifacial PV plants can contribute to active and reactive power sharing with the network to supply the load and improve the voltage profile. The network parameters and load data are derived from [14].

B. Results and discussions

Three operation scenarios were adopted to investigate the impacts of bifacial PV plants and compare their performance with their mono-facial counterparts; 1) Base case; without PV generations, 2) CVR strategy with mono-facial PVs, and 3) CVR strategy with bifacial PVs.

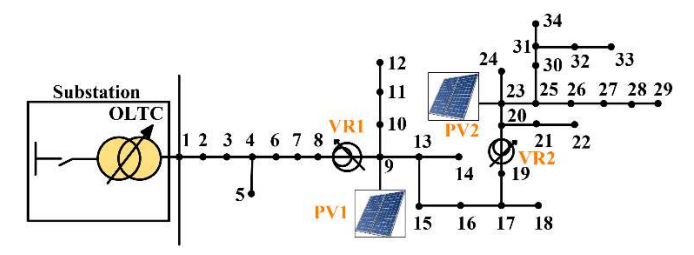


Fig. 6. Modified IEEE 34-bus system.

The amount of energy received from the substation as well as the power losses for the three scenarios are presented in Table 1. As can be observed, the network requires 23.3 MWh in the first scenario, considering that there is no PV power generation. This amount drops to 21.45 MWh in the second scenario, where mono-facial PV plants can generate power at their maximum capacity. Scenario 3 shows the least amount of energy received from the substation (19.9 MWh) as the bifacial provides more active power to meet the network demand.

TABLE I. ENERGY AND POWER LOSS FOR THE THREE SCENARIOS

	Energy (kWh)	Power Loss (kWh)
Scenario 1	23300	1970
Scenario 2	21450	1867
Scenario 3	19900	1810

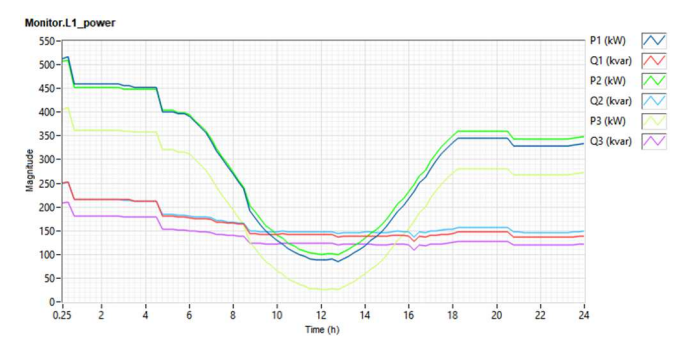


Fig. 7. Received active and reactive power from the substation for scenario 2 (with mono-facial PV systems).

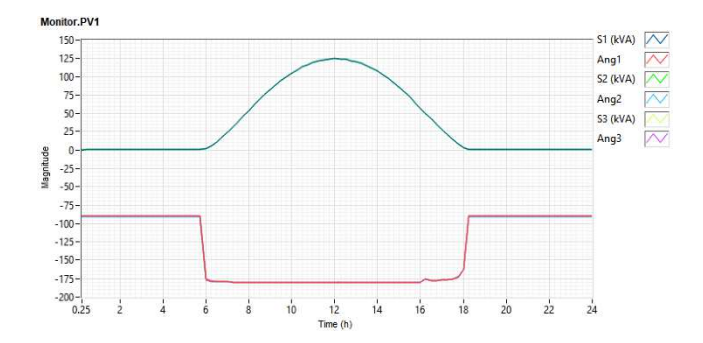


Fig. 8. Generated power by mono-facial PV systems (scenario 2)

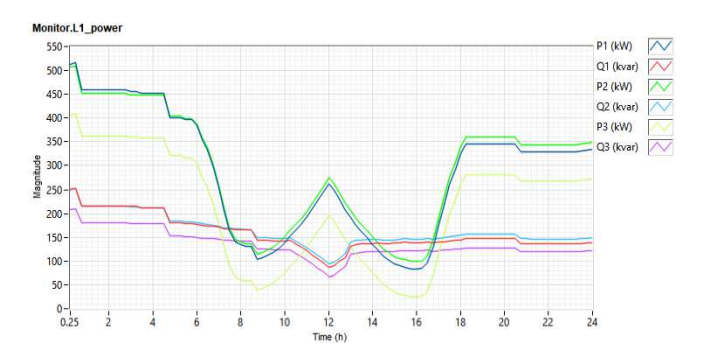


Fig. 9. Received active and reactive power from the substation for scenario 3 (with bifacial PV systems).

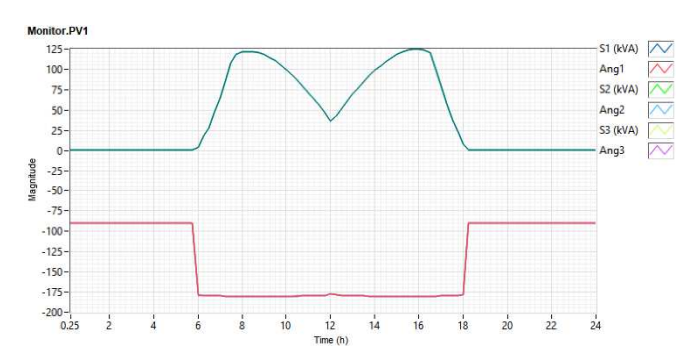


Fig. 10. Generated power by bifacial PV systems (scenario 3)

Fig. 7 demonstrates the active and reactive power received from the substation for the day-ahead planning for the second scenario, and the power generated by the mono-facial PVs are shown in Fig. 8. As can be seen, the conventional mono-facial PVs provide the maximum available power at midday which

coincides with the light load demand. A small decrease in load demand around noon has resulted in PVs over-generation. Fig. 9 depicts the active and reactive powers imported from the substation for the third scenario, and the power generated by the bifacial PVs is illustrated in Fig 10. It is evident that the substation power is determined based on the double-peak profile of the bifacial PVs. The peak demand in the 34-bus system happens in the morning. Thus, the morning humps of the bifacial PVs can alleviate the peak demand before noon. In general, by knowing the network characteristics (including the yearly load demand profile), PVs operators can adjust the PV modules (e.g., inclination (tilt) and orientation angles, the height off the ground, and the horizontal distance between PV rows) so that the maximum efficiency is obtained.

V. CONCLUSION

Bifacial PV systems generate extra power compared to their mono-facial counterparts. The two-humped profile of bifacial PVs can bring advantages for the distribution network operators. This double-peak profile almost coincides with the morning and evening peaks in power demand. This interesting feature helps the operators better deal with the abundance of renewable generation during midday. This paper introduced a new CVR framework that utilized the double-peak profile of bifacial PVs to optimize the operation of a distribution network. The approach was carried out via optimal coordination of OLTCs and VRs, as well as Volt/VAr control of smart inverters. The effectiveness of the proposed strategy was verified on the modified 34-bus system. The results showed the advantages of bifacial PVs over conventional mono-facial panels.

REFERENCES

- [1] Q. Zhang, K. Dehghanpour, and Z. Wang, "Distributed CVR in Unbalanced Distribution Systems With PV Penetration," *IEEE Transactions on Smart Grid*, vol. 10, no. 5, pp. 5308-5319, 2019.
- [2] F. Ding and M. Baggu, "Coordinated Use of Smart Inverters with Legacy Voltage Regulating Devices in Distribution Systems with High Distributed PV Penetration — Increase CVR Energy Savings," *IEEE Transactions on Smart Grid*, doi: 10.1109/TSG.2018.2857410.
- [3] S. Singh, S. Veda, S. P. Singh, R. Jain, and M. Baggu, "Event-Driven Predictive Approach for Real-Time Volt/VAR Control With CVR in Solar PV Rich Active Distribution Network," *IEEE Transactions on Power Systems*, vol. 36, no. 5, pp. 3849-3864, Sept. 2021.
- [4] M. S. Hossan and B. Chowdhury, "Integrated CVR and Demand Response Framework for Advanced Distribution Management Systems," *IEEE Transactions on Sustainable Energy*, vol. 11, no. 1, pp. 534-544, Jan. 2020.
- [5] L. Gutierrez-Lagos and L. F. Ochoa, "OPF-Based CVR Operation in PV-Rich MV-LV Distribution Networks," *IEEE Transactions on Power Systems*, vol. 34, no. 4, pp. 2778-2789, 2019.
- [6] S. Paul, A. Sharma and N. P. Padhy, "Risk Constrained Energy Efficient Optimal Operation of a Converter Governed AC/DC Hybrid Distribution Network With Distributed Energy Resources and Volt-VAR Controlling Devices," *IEEE Transactions on Industry Applications*, vol. 57, no. 4, pp. 4263-4277, 2021.
- [7] S. Singh, V. B. Pamshetti, and S. P. Singh, "Time Horizon-Based Model Predictive Volt/VAR Optimization for Smart Grid Enabled CVR in the Presence of Electric Vehicle Charging Loads," *IEEE Transactions on Industry Applications*, vol. 55, no. 6, pp. 5502-5513, 2019.
- [8] A. Singhal, V. Ajjarapu, J. Fuller, and J. Hansen, "Real-Time Local Volt/Var Control Under External Disturbances With High PV Penetration," *IEEE Transactions on Smart Grid*, vol. 10, no. 4, pp. 3849-3859, 2019.

- [9] R. R. Jha, A. Dubey, C. Liu and K. P. Schneider, "Bi-Level Volt-VAR Optimization to Coordinate Smart Inverters With Voltage Control Devices," *IEEE Transactions on Power Systems*, vol. 34, no. 3, pp. 1801-1813, 2019.
- [10] V. B. Pamshetti and S. P. Singh, "Coordinated Allocation of BESS and SOP in High PV Penetrated Distribution Network Incorporating DR and CVR Schemes," in *IEEE Systems Journal*, doi: 10.1109/JSYST.2020.3041013.
- [11] V. B. Pamshetti, S. Singh, A. K. Thakur, and S. P. Singh, "Multistage Coordination Volt/VAR Control With CVR in Active Distribution Network in Presence of Inverter-Based DG Units and Soft Open Points," *IEEE Transactions on Industry Applications*, vol. 57, no. 3, pp. 2035– 2047, 2021.
- [12] S. Singh, V. Babu Pamshetti, A. K. Thakur, and S. P. Singh, "Multistage Multiobjective Volt/VAR Control for Smart Grid-Enabled CVR With Solar PV Penetration," *IEEE Systems Journal*, vol. 15, no. 2, pp. 2767-2778, 2021.
- [13] M. Ahanch and R. McCann, "Integrated Volt/Var Control and Conservation Voltage Reduction in Unbalanced Distribution Networks Considering Smart PV Inverter Control Using Equilibrium Optimizer Algorithm," 2021 IEEE Kansas Power and Energy Conference (KPEC), 2021, pp. 1-6, doi: 10.1109/KPEC51835.2021.9446226.
- [14] M. Ahanch and R. McCann, "Implementation of CVR in Distribution Networks by Optimal Coordination of BESS and PV Inverters Using Arithmetic Optimization Algorithm," 2021 North American Power Symposium (NAPS), 2021, pp. 1-6, doi: 10.1109/NAPS52732.2021.9654489.
- [15] F. Toor and L. Research, "1/W system price: How bifacial modules will beat the needed efficiency and cost targets," 2nd Bifacial PV Workshop, Chambéry, France, May 2014.
- [16] X. Sun, M. R. Khan, C. Deline, and M. A. Alam, "Optimization and Performance of Bifacial Solar Modules: A Global Perspective," *Applied Energy*, vol. 212, pp. 1601-1610, 2018.
- [17] D. P. Simatupang and J. Choi, "Integrated Photovoltaic Inverters Based on Unified Power Quality Conditioner with Voltage Compensation for Submarine Distribution System," *Energies*, vol. 11, no. 11. MDPI AG, p. 2927, Oct. 26, 2018. doi: 10.3390/en11112927.

- [18] A. Balal, S. Dinkhah, F. Shahabi, M. Herrera, and Y. L. Chuang, "A Review on Multilevel Inverter Topologies," *Emerging Science Journal*, vol. 6, no. 1. Ital Publication, pp. 185–200, Feb. 01, 2022. doi: 10.28991/esj-2022-06-01-014.
- [19] A. Balal, M. Abedi, and F. Shahabi, "Optimized generated power of a solar PV system using an intelligent tracking technique," International Journal of Power Electronics and Drive Systems (IJPEDS), vol. 12, no. 4. *Institute of Advanced Engineering and Science*, p. 2580, Dec. 01, 2021. doi: 10.11591/ijpeds.v12.i4.pp2580-2592.
- [20] H. P. Yin et al., "Optical enhanced effects on the electrical performance and energy yield of bifacial PV modules," *Solar Energy*, vol. 217. Elsevier BV, pp. 245–252, 2021.
- [21] H. Nussbaumer, M. Klenk, M. Morf, and N. Keller, "Energy yield prediction of a bifacial PV system with a miniaturized test array," *Solar Energy*, vol. 179. Elsevier BV, pp. 316–325, 2019.
- [22] A. Asgharzadeh, B. Marion, C. Deline, C. Hansen, J. S. Stein, and F. Toor, "A Sensitivity Study of the Impact of Installation Parameters and System Configuration on the Performance of Bifacial PV Arrays," *IEEE Journal* of Photovoltaics, vol. 8, no. 3, pp. 798-805, 2018.
- [23] T. S. Liang et al., "A review of crystalline silicon bifacial photovoltaic performance characterization and simulation," Energy & Environmental Science, vol. 12, no. 1. Royal Society of Chemistry (RSC), pp. 116–148, 2019
- [24] M. Rouholamini, L. Chen, and C. Wang, "Modeling, Configuration, and Grid Integration Analysis of Bifacial PV Arrays," *IEEE Transactions on Sustainable Energy*, vol. 12, no. 2, pp. 1242-1255, 2021.
- [25] T. Gonen, Electric Power Distribution Engineering. CRC Press, 2015.
- [26] S. Arora, S. Satsangi, S. Kaur, and R. Khanna, "Substation demand reduction by CVR enabled intelligent PV inverter control functions in distribution systems," *Int Trans Electr Energ Syst*, vol. 31, no. 2, 2020.